High-order laser harmonics and synchrotron study of transition metals $M_{2,3}$ edges

R. Berlasso,[1] C. Dallera,[1] F. Borgatti,[2] C. Vozzi,[1] G. Sansone,[1] S. Stagira,[1] M. Nisoli,[1] G. Ghiringhelli,[1] P. Villoresi,[3] L. Poletto,[3] M. Pascolini,[3] S. Nannarone,[2,4] S. De Silvestri,[1] and L. Braicovich[1]

[1]*INFM - Dipartimento di Fisica, Politecnico di Milano, piazza L. da Vinci 32, 20133 Milano, Italy*

[2]*TASC-INFM Area Science Park, Basovizza, Building MM, S.S. 14, Km. 163.5, I-34012, Trieste, Italy*

[3]*INFM - DEI, Università di Padova, Via Gradenigo 6a, 35131 Padova, Italy*

[4]*Dipartimento di Ingegneria dei Materiali e dell'Ambiente, Università di Modena e Reggio Emilia, Via Vignolese 905, 41100 Modena, Italy*

(Received 5 July 2005; revised manuscript received 29 November 2005; published 1 March 2006)

We report on a study of *M* edges of transition metals and their oxides performed by using high-order harmonics of ultrafast laser pulses and synchrotron radiation. Data of the Mn, Fe, and Co 3*p* edges demonstrate that laser harmonics in the extreme ultraviolet range are suited for spectroscopy of solids. These results open perspectives for measurements which could in the future be performed in time-resolved mode. Resonant reflectivity of Fe, Co, Fe_2O_3, and CoO measured at the synchrotron complements the experiment by providing the detailed line shape of the refraction index for reference.

DOI: 10.1103/PhysRevB.73.115101 PACS number(s): 78.20.Ci, 78.40.Kc, 78.70.Dm, 78.47.+p

I. INTRODUCTION

Intense and collimated pulses of femtosecond time duration are nowadays readily available from laser sources. High-order harmonic generation (HHG) of the fundamental radiation produces photons that reach into the extreme ultraviolet (XUV) range.[1] The use of harmonic radiation as a spectroscopic tool presents appealing possibilities for "pump-and-probe" experiments in an almost unexplored energy range, with a time resolution well ahead of the most modern synchrotron sources. In this work we present 3*p* edge transmission and resonant reflectivity of some TMs performed with a high order harmonic source. We demonstrate the possibility of reflection and absorption spectroscopy in the XUV range with such ultrafast source. The experiment included a run by synchrotron radiation (SR) on the same samples and in the same energy range. The parallel use of SR complemented and reinforced the results obtained by the use of high order harmonics mainly compensating the intrinsic noncontinuous photon energy distribution of that source. The overall agreement of the results demonstrates the feasibility of this approach. Our experiment did not include temporal analysis as yet, but puts the premises for time resolved XUV studies of solids in the femtosecond domain, performed with a laboratory table-top equipment: the use of harmonic radiation as a spectroscopic tool presents appealing possibilities for probing matter properties both in the spectral and in the temporal domain. Our present measurements give us the basis for discussing the limitations and unique aspects of experiments performed with HHG radiation.

II. TRANSMISSION AND REFLECTIVITY MEASUREMENTS WITH HIGH ORDER HARMONICS

Absorption and reflectivity spectra of Mn, Fe, and Co were measured using XUV radiation produced by HHG. Harmonic radiation was produced focusing 25 fs light pulses, generated by a Ti:sapphire laser system (800 nm≡1.5 eV central wavelength, 1 kHz repetition rate) into a neon jet.[2] An Al filter blocked the fundamental radiation and limited the maximum photon energy to ~70 eV. To observe the harmonic emission we used a high-resolution flat-field spectrometer and a high-resolution CCD detector.[3] Absorption was first measured in transmission mode. To this purpose we evaporated ~55 Å of Fe on a 0.1-μm-thick parylene substrate backed by a Ni mesh. The sample was mounted in vacuum (~10^{-6} mbar). Transmission through the Fe-on-parylene sample and through the bare parylene substrate was measured by alternately acquiring the direct and transmitted harmonics. The harmonics spectrum before and past the Fe sample is shown in Fig. 1(a), rescaled to the same height for comparison (the spectrum of transmitted harmonics was multiplied by 5). Each spectrum is the average over ~500 laser pulses. Only the odd harmonics are present in the spectrum, and the peaks are therefore spaced by 3 eV. The effect of Fe *M* edge absorption is clear from the depression of the harmonics at ~58 eV. Also shown in Fig. 1(a) is the trend of the quantity $\mu(\omega)\times d$, obtained through the relation $I_t(\omega) = I_0(\omega)\times\exp[-\mu(\omega)\times d]$, where $I_0(\omega)$ is the incident light intensity, $I_t(\omega)$ the transmitted intensity, d the sample thickness, and $\mu(\omega)$ the absorption coefficient. The curves were sampled in correspondence of the peak position and of two adjacent points, where the beam intensity I_0 is sufficiently intense to make the ratio I_t/I_0 meaningful. We compared for reference our measured data with those obtained from the *Center for X-Ray Optics* Berkeley database,[4] namely, in Fig. 1(a) the quantity $\mu(\omega)\times d$ for Fe on parylene, in Fig. 1(b) the Fe absorption (after subtraction of the parylene signal), in Fig. 1(c) transmission through Fe and parylene. A very good overall agreement is found for each set of curves.

Transmission measures directly the absorption coefficient and gives access to the complex refraction index but with the drawback of restriction to samples of suitable thickness. Reflectivity provides—through Kramers-Kronig (KK) relations[5]—the same information though without such limitation. We measured reflectivity spectra of polished Fe, Co

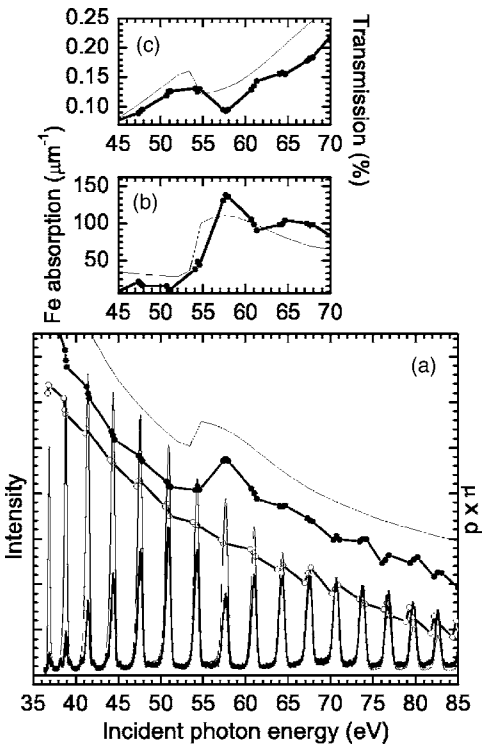

FIG. 1. Transmission spectrum of Fe measured with harmonic radiation. (a) Direct harmonic spectrum (thin line) and harmonics after transmission through 55 Å Fe on 0.1 μm parylene (thick line). The dotted curves represent the quantity $\mu(\omega)\times d$ for the parylene substrate (hollow dots), and for the Fe on parylene sample (black dots) [for the Fe on parylene sample $\mu(\omega)\times d$ is the sum of two terms, for Fe and parylene, respectively]. The thin line is taken from the CXRO database (vertically offset for clarity). The right axis refers to the latter three curves. (b) Absorption spectrum of Fe only (dots), compared with CXRO spectrum (line). (c) Transmission through Fe and parylene (dots) compared with CXRO curves (line).

monocrystals and of a Mn flake using the same laser source, coupled to a similar grating spectrometer.[6] Two flat, Pt coated mirrors of x-ray quality were used to deviate the beam onto the sample, and to bring the reflected beam back into the original path. The incidence angle was $\sim 8°$ with respect to the sample surface. Spectra with and without the sample were alternated, with an integration time of 1 s. The results presented in Fig. 2 are averaged over 10 s and each spectral point is the ratio of the integrated intensity of reflected and direct harmonics. The consequent 3 eV point spacing does not allow to unveil fine spectral details, but in pump-and-probe experiments we will aim at monitoring the intensity changes at selected energies. Also, comparison with SR spectra measured by us on Fe and Co (Fig. 2), shows rather unstructured line shapes in this case.

The results obtained with the XUV laser harmonics open perspectives in the field of resonant spectroscopies, but at this point it is also obvious that spectroscopy performed with HHG radiation suffers from two main factors, namely, the moderate photon flux and the noncontinuous spectral intensity. The latter problem presents two aspects: HHG with high spectral purity and large tunability can be obtained using a subnanosecond tunable driving pulse, providing a suitable

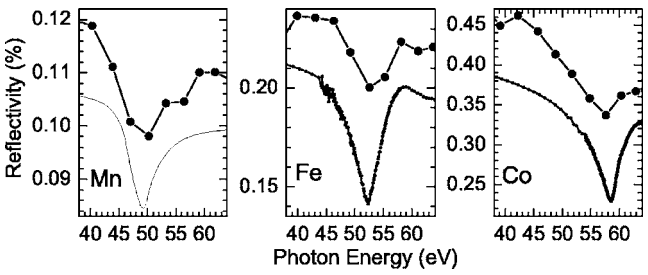

FIG. 2. Reflectivity spectra measured with harmonic radiation (big dots) compared with CXRO curves (continuous line, for Mn) and with our SR data at 10° incidence from the sample surface (small dots, curves for Fe and Co as in Fig. 3). CXRO and SR spectra were rescaled to match the smaller values of harmonic reflectivity due to stronger roughness.

source for investigations in the XUV spectral domain,[7] but at the expense of a longer time duration of the pulses. On the other hand, ultrashort pulses generated by femtosecond laser sources can provide an ideal tool for pump-probe experiments.[8] Femtosecond sources are, however, less adapted to spectral tunability, that can still be achieved by tailoring the generating conditions, i.e., the density of the generating medium or the driving pulse intensity,[9] the interaction geometry[10] or the shape of the driving pulse in the temporal domain by adaptive techniques.[11] A special mention goes to HHG by near single-cycle laser pulses, which allows the generation of attosecond XUV pulses[12] with continuous spectrum. This implies a more complex setup (optical compression[13] and stabilization of the carrier-envelope phase[14]), and gives rise to a continuum spectrum only in the weak cutoff region.

As concerns the photon flux, to our best estimate the HHG source yielded 10^5 photons/pulse, at 1 kHz frequency, integrated over one harmonic in the plateau region, leading to a flux of 10^8 ph/s per harmonic (~ 1 eV wide). For comparison, the photon flux of the SR experiment presented hereafter amounted (at the same energies) to 10^9 ph/s in a bandwidth of 0.02 eV.

The lower intensity of HHG radiation obviously limits the possibility of exploring different experimental parameters. Characteristics such as the polarization are nevertheless object of research: XUV radiation by HHG is commonly generated by linearly polarized beams, and retains the polarization state of the driving pulses. Since spectroscopic investigations concerned with the magnetization dynamics could benefit from the generation of elliptically polarized XUV pulses, HHG techniques based on the interaction of multiple laser pulses with different polarization and central frequency have been investigated from the experimental[15] and theoretical[16] point of view. Such techniques generate XUV pulses with nonlinear polarization state, still with reasonable yields. The existing results overall thus indicate that efforts towards the use of HHG as an effective spectroscopic tool are progressing. Time-resolved studies with HHG could provide access to an enormous variety of physical information: the time evolution of the electronic interactions in strongly correlated materials (e.g., heavy fermions), the exploration of the magnetization, and structural dynamics of

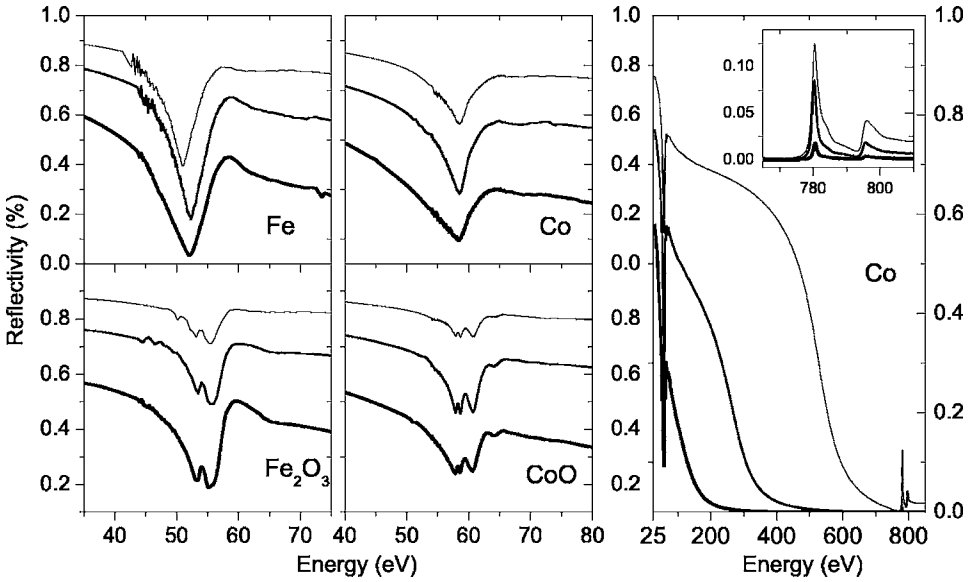

FIG. 3. M and L edge SR reflectivity at grazing incidence of 5° (thin line), 10° (medium line), 20° (thick line). The right most panel displays Co reflectivities extended by using CXRO data. Co L spectra shown in the inset (spectra at 20° multiplied by 100, at 10° by 10).

solids are only few examples of studies that have been performed up to now with optical and infrared radiation.[17–19] Time-resolved experiments performed with XUV beams will add the element sensitivity of core spectroscopies.

III. REFLECTIVITY MEASUREMENTS WITH SYNCHROTRON RADIATION

The present study is completed by SR reflectivity data, whose more detailed shape allowed a solid KK analysis to yield the absorption curves. Resonant reflectivity of Fe, Co, Fe_2O_3, and CoO single crystals was measured at the bending magnet beamline BEAR (Ref. 20) at Elettra. Fe and Co surfaces were cleaned in vacuum (base pressure $\sim 2 \times 10^{-10}$ mbar) by sputtering and annealing, the oxides were cleaved prior to insertion in vacuum. M and L edge reflectivity of the TMs was measured at grazing incidence angles $(5°, 10°, 20°)$ with linear polarized light in s incidence. The resolving power $E/\Delta E$ was $\sim$5000 in the M edge region (50–70 eV) and $\sim$3000 at the L edges (700–900 eV). Reflected and incident intensities were measured by an absolute AXUV100-IRD diode and normalized using the current drained by a W mesh inserted in the light beam. Typical photodiode signals ranged from few nA at the M edge to 20–200 pA at the L edge. From the measured reflectivities we retrieved the optical constants through Kramers-Kronig transformation.[5]

The modulus of the reflectance $\hat{r}(\omega)=\sqrt{R(\omega)}e^{i\phi(\omega)}$ is directly obtained from the experiment [$R(\omega)$ is the measured reflectivity]. The KK integral transform provided the phase $\phi(\omega)$ of the reflectance[21]

$$\phi(\omega) = \frac{\omega}{\pi}\int_0^\infty \frac{\ln \frac{R(\omega')}{R(\omega)}}{\omega^2 - \omega'^2} d\omega' \tag{1}$$

and from $\hat{r}(\omega)$ we obtained the complex refractive index $N(\omega)=n(\omega)+ik(\omega)$ through Fresnel formula

$$\hat{r}(\omega) = \frac{\sin\theta - \sqrt{N(\omega)^2 - \cos^2\theta}}{\sin\theta + \sqrt{N(\omega)^2 - \cos^2\theta}} \tag{2}$$

(θ is the incidence angle from the sample surface).

We extended the measured spectra over the 0–30 keV range[22] as required from the integration domain of the KK transform (0 to ∞). Since the Fresnel expression is valid only for perfectly smooth surfaces, we retrieved the zero-roughness spectrum from the measured data through the Nevot-Croce[23] (NC) formalism.

Figure 3 shows the $M_{2,3}$ edge curves (four left panels). The spectral line shapes of Co, corrected for roughness and extended from 0 to 30 keV, are shown in the region of interest in Fig. 3 (see right panel: the inset shows the $L_{2,3}$ reflectivities of Co as example). The curves were feeded into the KK transform that yielded the n and k spectra of Fig. 4.

The complex refractive index N provides information about the electronic population and gives direct access to the absorption coefficient $\mu(\omega)=4\pi k(\omega)/\lambda$. The M edges of TMs have been studied in a limited number of cases,[24–35] the stronger $L_{2,3}$ absorption edges being more often exploited. M edge absorption however gives direct information on the coupling of $3p$ electrons to $3d$ valence states, which is a key data to the understanding of the electronic interactions. Solid state effects are responsible for the broad spectral shapes of Co and Fe, that is dominated by the width of the large $3d$ density of states. In the oxides the $3d$ electron wave function is localized by the large $3p$-$3d$ interaction, and the small width of the $3d$ oxide band allows to interpret the M absorption spectra in an atomic model. The lower panels of Fig. 4 compare measured data of Fe_2O_3 and CoO with spectra computed in the atomic multiplet approach.[36] The overall agreement shows that the atomic approach can describe the M edges of oxides well, even if some adjustment of the parameters with respect to L edges may be required. Details about the calculations are given at the end of the paper.

IV. CONCLUSIONS

In conclusion we have measured transmission and reflectivity spectra of $3d$ TMs core levels by high-order harmonics

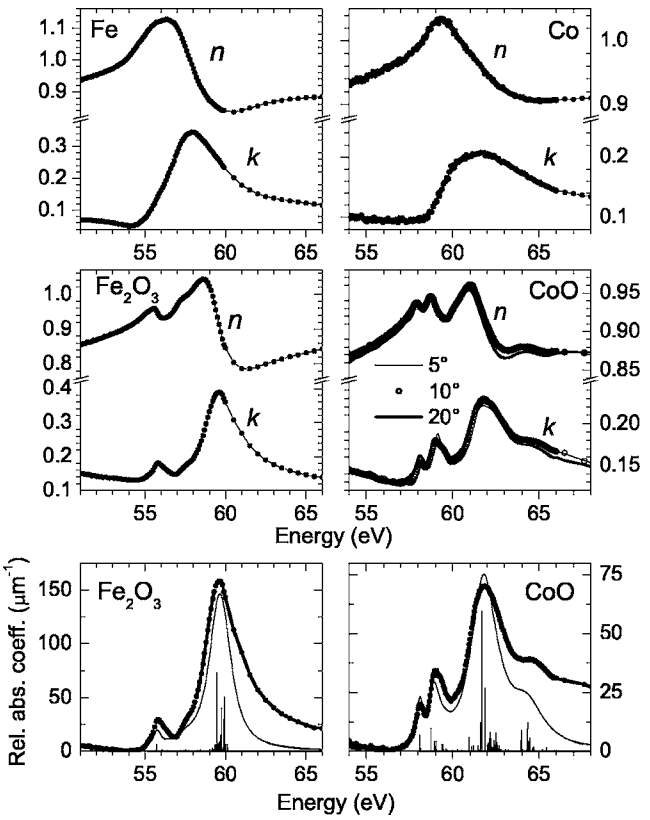

FIG. 4. Upper panels: Refractive index $N(\omega)=n(\omega)+ik(\omega)$, obtained from reflectivity spectra at 20°. The typical agreement from reflectivities at different angles is shown for CoO. Lower panels: Fe_2O_3, and CoO M edge absorption (absolute values relative to preedge): spectra obtained from reflectivity (dotted line) compared to atomic calculation (continuous line, sticks are electronic states before broadening).

of fs laser pulses and SR. The laser study shows that resonant spectroscopy can be performed with table-top equipment and are a step towards studies of ultrafast electronic dynamics with the selectivity of core spectroscopies. The curves obtained by SR are a reference useful to the physical interpretation of the line shapes. The planned studies of laser spectroscopies will concentrate on the change of the spectral intensity at relevant energies. We foresee that such studies will add crucial information to the time evolution of the interactions of electronic and lattice degrees of freedom of the solids.

ACKNOWLEDGMENTS

We thank A. Giglia, N. Mahne, and M. Pedio for support in the experiment. C.D. wishes to thank A. Perucchi and L. Degiorgi for useful hints on the use of KK relations. The contribution of R. Gusmeroli for the atomic calculation is acknowledged. This work was partially supported by European Union under Project No. MRTN-CT-2003-505138 (XTRA).

APPENDIX: ATOMIC MULTIPLET CALCULATION DETAILS

An atomic Hartree-Fock calculation[37] gives the $3d$-$3d$ and $3d$-$3p$ Coulomb and exchange interactions for initial $3d^5$ ($3d^7$ for Co^{2+}) and final $3p^53d^6$ ($3p^53d^8$ for Co^{2+}) configurations. An octahedral crystal field is accounted for through the parameter $10Dq$. For Fe^{3+} we adopted a $10Dq$ of 1.45 eV as in Ref. 38, for Co^{2+} the best fit was obtained for $10Dq=0.9$ eV (similar to the 1 eV value at the L edge in Ref. 39). To match the experimental data we reduced the Slater parameters to 50% of their value, instead of the usual 80% that accounts for intra-atomic screening effects for L absorption spectra of oxides.[40] This unusual scaling may derive only marginally from neglecting the charge-transfer configuration $3d^6L^{-1}$ ($3d^8L^{-1}$ for Co^{2+}), where L^{-1} is a hole in the oxygen ligand, and is mainly required by the smaller $3d$ shell collapse induced by the $3p$ core hole with respect to the $2p$ core hole. In fact it was not needed in the L edge spectra calculation of Ref. 38. The spectra were broadened by Lorentzians of increasing HWHM along the spectrum: from 0.1 to 0.9 eV for Fe^{3+}, from 0.05 to 1 eV for Co^{2+}. These values were chosen phenomenologically and reflect the presence of additional decay channels. Convolution with a Gaussian (FWHM=0.15 eV) simulates the resolution function.

[1] E. A. Gibson, A. Paul, N. Wagner, R. Tobey, D. Gaudiosi, S. Backus, I. P. Christov, A. Aquila, E. M. Gullikson, D. T. Attwood, M. M. Murnane, and H. C. Kapteyn, Science **302**, 95 (2003).

[2] M. Nisoli, E. Priori, G. Sansone, S. Stagira, G. Cerullo, S. De Silvestri, C. Altucci, R. Bruzzese, C. de Lisio, P. Villoresi, L. Poletto, M. Pascolini, and G. Tondello, Phys. Rev. Lett. **88**, 033902 (2002).

[3] L. Poletto, G. Tondello, and P. Villoresi, Rev. Sci. Instrum. **72**, 2868 (2001).

[4] Berkeley Center for X-ray Optics, http://www-cxro.lbl.gov

[5] L. Landau and E. Lifshits, *Electrodynamics of Continuous Media* (Pergamon, London, 1960).

[6] L. Poletto, S. Bonora, M. Pascolini, and P. Villoresi, Rev. Sci. Instrum. **75**, 4413 (2004).

[7] F. Brandi, D. Neshev, and W. Ubachs, Phys. Rev. Lett. **91**, 163901 (2003).

[8] S. Dobosz, G. Doumy, H. Stabile, P. D'Oliveira, P. Monot, F. Réau, S. Hüller, and P. Martin, Phys. Rev. Lett. **95**, 025001 (2005).

[9] C.-G. Wahlström, J. Larsson, A. Persson, T. Starczewski, S. Svanberg, P. Salières, P. Balcou, and A. L'Huillier, Phys. Rev. A **48**, 4709 (1993).

[10] C. Altucci, R. Bruzzese, C. de Lisio, M. Nisoli, S. Stagira, S. De Silvestri, O. Svelto, A. Boscolo, P. Ceccherini, L. Poletto, G. Tondello, and P. Villoresi, Phys. Rev. A **61**, 021801(R) (1999).

[11] D. H. Reitze, S. Kazamias, F. Weihe, G. Mullot, D. Douillet, F. Aug, O. Albert, V. Ramanathan, J. P. Chambaret, D. Hulin, and P. Balcou, Opt. Lett. **29**, 86 (2004).

[12] M. Hentschel, R. Kienberger, C. Spielmann, G. A. Reider, N.

Milosevic, T. Brabec, P. Corkum, U. Heinzmann, M. Drescher, and F. Krausz, Nature (London) **414**, 509 (2001).
[13] M. Nisoli, S. D. Silvestri, and O. Svelto, Appl. Phys. Lett. **68**, 2793 (1996).
[14] A. Apolonski, A. Poppe, G. Tempea, C. Spielmann, T. Udem, R. Holzwarth, T. W. Hänsch, and F. Krausz, Phys. Rev. Lett. **85**, 740 (2000).
[15] H. Eichmann, A. Egbert, S. Nolte, C. Momma, B. Wellegehausen, W. Becker, S. Long, and J. K. McIver, Phys. Rev. A **51**, R3414 (1995).
[16] D. B. Milosevic, W. Becker, and R. Kopold, Phys. Rev. A **61**, 063403 (2000).
[17] K. H. Ahn, M. J. Graf, S. A. Trugman, J. Demsar, R. D. Averitt, J. L. Sarrao, and A. J. Taylor, Phys. Rev. B **69**, 045114 (2004).
[18] M. Vomir, L. H. F. Andrade, L. Guidoni, E. Beaurepaire, and J.-Y. Bigot, Phys. Rev. Lett. **94**, 237601 (2005).
[19] A. Cavalleri, T. Dekorsy, H. H. Chong, J. C. Kieffer, and R. W. Schoenlein, Phys. Rev. B **70**, 161102(R) (2004).
[20] S. Nannarone, F. Borgatti, A. DeLuisa, B. P. Doyle, G. C. Gazzadi, A. Giglia, P. Finetti, N. Mahne, L. Pasquali, M. Pedio, G. Selvaggi, G. Naletto, M. G. Pelizzo, and G. Tondello, in *Synchrotron Radiation Instrumentation: Eighth International Conference on Synchrotron Radiation Instrumentation*, edited by Tong Warwick *et al.*, AIP Conf. Proc. No. 705 (AIP, Melville, 2004), p. 450.
[21] F. Wooten, *Optical Properties of Solids* (Academic Press, New York, 1972).
[22] We used reflectivity curves from the Berkeley CXRO database (Ref. 4) above 30 eV. Below 30 eV, for Fe and Co we used data of Ref. 41 for the 1 to 30 eV range and the Hagen-Rubens analytical extension (Ref. 42) ($[1-R(\omega)] \propto \omega^{-1/2}$) for metals below 1 eV. For CoO Ref. 43 covers the 0–26 eV energy range (insulators have a constant reflectivity for $\omega \to 0$). No data were available for the low-energy region of Fe_2O_3, but we could check in all other cases that, for a wide enough integration range, the exact shape of the 0–30 eV extension does not affect the KK results above 50 eV. The local behavior of KK transform allowed us to neglect the oxygen *K* edge in the extended curves.
[23] L. Nevot and P. Croce, Rev. Phys. Appl. **15**, 761 (1980). In the Nevot-Croce model (also employed by the CXRO database) the reflectivity R_0 and R of the flat and rough sample are related by $R_0 = R \exp[(2\omega \sin\theta\sigma/\hbar c)^2]$ (σ is the root mean square of the vertical interface roughness, θ the angle from the surface). The σ values were chosen using reflectivity at *L* edges, where the strong effect of roughness makes its choice unique. We find $\sigma = 0.365$ nm for Fe, 0.3 nm for Fe_2O_3, 0.45 nm for Co, and 0.5 nm for CoO.
[24] B. Sonntag, R. Haensel, and C. Kunz, Solid State Commun. **7**, 597 (1969).
[25] F. C. Brown, C. Gähwiller, and A. B. Kunz, Solid State Commun. **9**, 487 (1971).
[26] S. Nakai, H. Nakamori, A. Tomita, K. Tsutsumi, H. Nakamura, and C. Sugiura, Phys. Rev. B **9**, 1870 (1971).
[27] L. C. Davis and L. A. Feldkamp, Solid State Commun. **19**, 413 (1976).
[28] R. Bruhn, B. Sonntag, and H. W. Wolff, J. Phys. B **12**, 203 (1979).
[29] H. Onuki and J. C. Rife, Phys. Rev. B **26**, 654 (1982).
[30] A. Fujimori, M. Saeki, N. Kimizuka, M. Taniguchi, and S. Suga, Phys. Rev. B **34**, 7318 (1986).
[31] T. Koide, T. Shidara, H. Fukutani, K. Yamaguchi, A. Fujimori, and S. Kimura, Phys. Rev. B **44**, 4697 (1991).
[32] G. van der Laan, J. Phys.: Condens. Matter **3**, 7443 (1991).
[33] T. Koide, T. Shidara, K. Yamaguchi, A. Fujimori, H. Fukutani, N. Kimizuka, and S. Kimura, J. Electron Spectrosc. Relat. Phenom. **78**, 275 (1996).
[34] M. Sacchi, G. Panaccione, J. Vogel, A. Mirone, and G. van der Laan, Phys. Rev. B **58**, 3750 (1998).
[35] N. D. Telling, A. Haznar, G. van der Laan, M. D. Roper, F. Schedin, and G. Thornton, Physica B **345**, 157 (2004).
[36] G. van der Laan and B. T. Thole, Phys. Rev. B **43**, 13401 (1991).
[37] R. Cowan, *The Theory of Atomic Structure and Spectra* (University of California Press, Berkeley, CA, 1981).
[38] P. Kuiper, B. G. Searle, P. Rudolf, L. H. Tjeng, and C. T. Chen, Phys. Rev. Lett. **70**, 1549 (1993).
[39] F. M. F. de Groot, M. Abbate, J. van Elp, G. A. Sawatzky, Y. J. Ma, C. T. Chen, and F. Sette, J. Phys.: Condens. Matter **5**, 2277 (1993).
[40] F. M. F. de Groot, J. C. Fuggle, B. T. Thole, and G. A. Sawatzky, Phys. Rev. B **42**, 5459 (1990).
[41] J. Weaver, C. Krafka, D. Lynch, and E. Koch, *Optical Properties of Metals*, edited by H. Behrens and G. Ebel (Fachinformationszentrum Energie, Physik, Mathematik GmbH, Karlsruhe, 1981).
[42] M. Dressel and G. Grüner, *Electrodynamics of Solids* (Cambridge University Press, Cambridge, 2002).
[43] R. J. Powell and W. E. Spicer, Phys. Rev. B **2**, 2182 (1970).